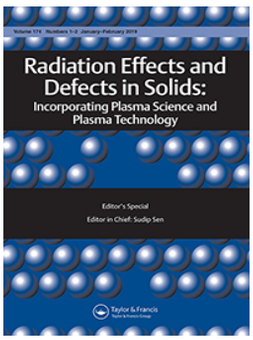

Taylor & Francis
Taylor & Francis Group

Radiation Effects and Defects in Solids
Incorporating Plasma Science and Plasma Technology

ISSN: 1042-0150 (Print) 1029-4953 (Online) Journal homepage: https://www.tandfonline.com/loi/grad20

MHD equilibria with magnetic islands in the TJ-II heliac

L. Benjamín Centurión & Julio J. Martinell

To cite this article: L. Benjamín Centurión & Julio J. Martinell (2019) MHD equilibria with magnetic islands in the TJ-II heliac, Radiation Effects and Defects in Solids, 174:1-2, 9-18, DOI: 10.1080/10420150.2019.1577854

To link to this article: https://doi.org/10.1080/10420150.2019.1577854

Published online: 02 Apr 2019.

RADIATION EFFECTS & DEFECTS IN SOLIDS
2019, VOL. 174, NOS. 1–2, 9–18
https://doi.org/10.1080/10420150.2019.1577854

Taylor & Francis
Taylor & Francis Group

MHD equilibria with magnetic islands in the TJ-II heliac

L. Benjamín Centurión and Julio J. Martinell

Instituto de Ciencias Nucleares, UNAM, México D.F., Mexico

ABSTRACT

Magnetic islands normally form at the low-order magnetic rational surfaces in toroidal confinement systems when a symmetry-breaking perturbation arises. In stellarators, the equilibrium state for the plasma once the perturbation has created the islands is not easy to describe due to its complexity. Numerical computation of equilibria can be done following a variational principle that minimizes the energy under given boundary constraints when no islands are allowed, as the VMEC code does. Islands can be included by adding helical perturbations and allowing magnetic field line slipping, which was incorporated in the SIESTA code. Here we use these two codes for the TJ-II heliac in order to compute the MHD equilibrium state that provides the environment for the occurrence of all other plasma processes. The computation was done in two parts, first, obtain an equilibrium with VMEC for the whole toroidal cycle and second, superimpose the magnetic islands to obtain a final equilibrium with SIESTA by adjusting the appropriate parameters.

ARTICLE HISTORY
Received 4 December 2018
Accepted 30 January 2019

KEYWORDS
MHD Equilibrium; toroidal confinement; magnetic islands

1. Introduction

Experiments in some stellarators have shown a correlation between the position of magnetic rational surfaces and energy transport reduction. In TJ-II, the electron temperature profile is observed to be modified around some low-order magnetic surfaces (*1*), in low density Electron Cyclotron Resonance heated discharges, while in LHD a sheared radial electric field is observed at the boundary of a magnetic island giving rise to heat transport reduction (*2*). Other studies based on Neutral Beam Injection in TJ-II discharges, produced a sweeping of the rational surfaces along the minor radius by varying the helical current, thus showing that the transport was consistently reduced at the position of the rational surfaces (*3*). Bolometry studies have also shown a correlation between transport barriers appearing on rational surfaces and MHD activity (*4*), which is expected to be related to magnetic island dynamics. Transport barriers around rational surfaces may also lead to confinement transitions of the L-H type. The natural association of magnetic islands with rational surfaces due to the resonance of the magnetic perturbations there, points to the importance of magnetic islands in the behavior of the plasma and in the context of confinement improvement.

In order to study the influence of islands on the plasma as a whole it is necessary to know the MHD equilibrium state with the presence of magnetic islands. This is a task that is

CONTACT Julio J. Martinell martinel@nucleares.unam.mx

not easy to accomplish since the MHD equilibrium in toroidal devices is usually computed under the assumption of nested magnetic surfaces. This is true for the VMEC equilibrium code (*5*) which uses a variational method to find the magnetic equilibrium given the vacuum magnetic fields at the prescribed boundary and the pressure and current (or iota) profiles. The equilibrium with internal flux tubes representing the magnetic islands can be computed with a different code named SIESTA which takes the VMEC equilibrium and imposes helical perturbations that resonate at the rational surfaces (*6*).

In this work, the VMEC - SIESTA code combination is used to calculate MHD equilibria with magnetic islands in the TJ-II geometry to determine the properties of the equilibrium islands. The starting equilibrium state is the one obtained by the VMEC code with nested magnetic surfaces taking the full toroidal range, as opposed to previous computations that used the heliac's toroidal symmetry of four periods. The standard procedure computed the equilibrium in just a single leg to reduce the code runtime and assumed a four time repetition to complete the full toroidal angle. However, doing this limits the toroidal periodicity of the islands computed later with SIESTA to multiples of four in toroidal number. This limitation was solved by tailoring the input parameters to extend VMEC running to cover the four-period cycle but keeping the same boundaries as before. In this way, running SIESTA with the new equilibria, magnetic islands of any periodicity are obtained, including those resonant at $\iota = 3/2$ whose magnetic islands were previously absent from the simulations. The results also show 2D pressure profiles that match the location of the magnetic islands observed in the Poincaré plots of the field lines.

The paper is organized as follows. In Section 2 the method for obtaining the MHD equilibrium with no islands over the complete toroidal range is described and the results are shown to be the same as when the periodicity is assumed. Section 3 then introduces the islands as perturbations to the initial MHD equilibrium. The difficulties in achieving a good convergence are described and present results for the magnetic field lines as well as the pressure distribution showing, in some cases, the presence of well formed islands. In Section 4 it is shown that in absence of imposed perturbations narrow islands can still be formed indicating the unstable nature of some of the VMEC equilibria. Finally, in the last section the conclusions of the work are presented.

2. VMEC equilibrium with no imposed toroidal symmetry

In order to allow the presence of magnetic islands of any periodicity in toroidal and poloidal directions we used the VMEC code in a way that computes the full range of toroidal angles. This produces MHD equilibrium states that can be used as starting points for later computations with any type of perturbations, in particular for creating magnetic islands of arbitrary periodicity at any rational surface using SIESTA code. The magnetic islands develop at the rational surface where the rotational transform ι is in resonance with a perturbation with toroidal mode number n and poloidal mode number m, i.e. $\iota = n/m$. We point out that the usual way of computing the equilibrium state in TJ-II was to take advantage of the periodic structure of the machine in toroidal direction, and obtain the fields for only one of the four legs, to reduce the code runtime. The total field is then given by repeating the same structure four times. While this is useful for most applications of the MHD equilibrium, it is not adequate when magnetic islands with periods that do not fit into the one-fourth length are to be formed. For instance, if the $\iota = 3/2$ rational is present in the equilibrium, a resonant

perturbation with $n = 3$ could give rise to an island but this would not be possible if the computed field structure only allows a periodicity $n = 4$ or multiples thereof.

The main modification made to VMEC was to change the assumed heliac's symmetry of 4 toroidal field periods (NFP = 4) to a single one (NFP = 1), multiplying the number of toroidal modes by four and modifying the corresponding mode amplitudes accordingly. Naturally, the goal is to get the same type of equilibrium with four toroidal periods but without imposing the periodicity from the outset. Some input parameters of VMEC had to be also modified, notably the minimum number of grid nodes in both directions. If this number cannot be satisfied the code fails to converge. The relations between the number of modes (MPOL and NTOR) and the minimum of grid nodes found to produce good convergence was NTHETA = 2 MPOL + 6 and NZETA = 2 NTOR + 4 + (1). The extra number (1) was added because it was necessary to get good results. The definition of the magnetic axis in terms of Fourier harmonics had also to be modified by increasing their number by four. The result of the computations for the TJ-II magnetic configuration 100_44_64 is shown in Figure 1 where it can be appreciated that the shape of the plasma has a toroidal periodicity of four when running the code with NFP = 1, thus confirming that the toroidal periodicity of the machine was kept the same. The whole magnetic equilibrium is actually the same as when NFP = 4. As a consequence, the rotational transform profiles are practically the same for both cases as seen in Figure 2. This is the most important feature for our study since it is what characterizes the magnetic surfaces regarding the formation of magnetic islands.

We worked with two TJ-II configurations that are commonly used in TJ-II: configuration 100_44_64 will be referred to as Case A, configuration 100_36_62 as Case B. For the

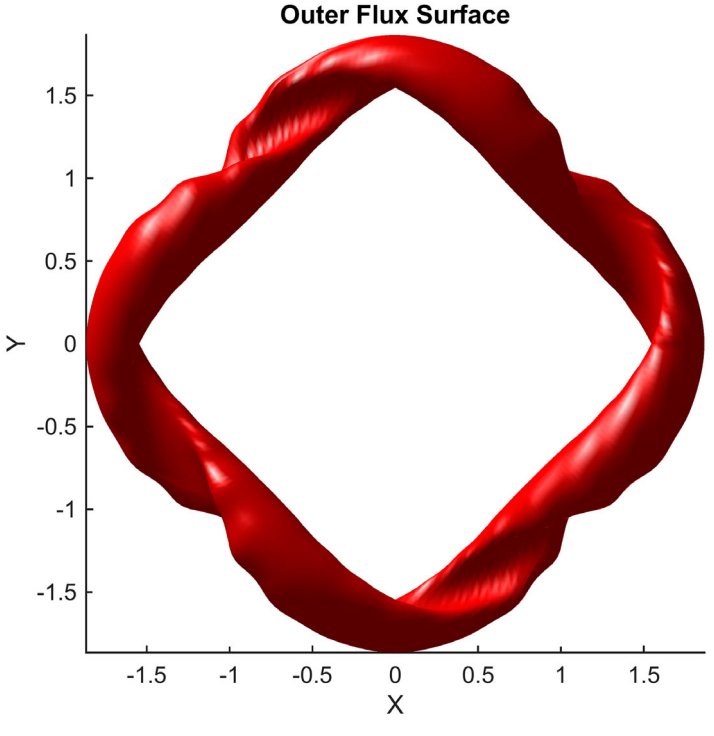

Figure 1. 3D external magnetic surface from VMEC for case A obtained with one field period (NFP = 1).

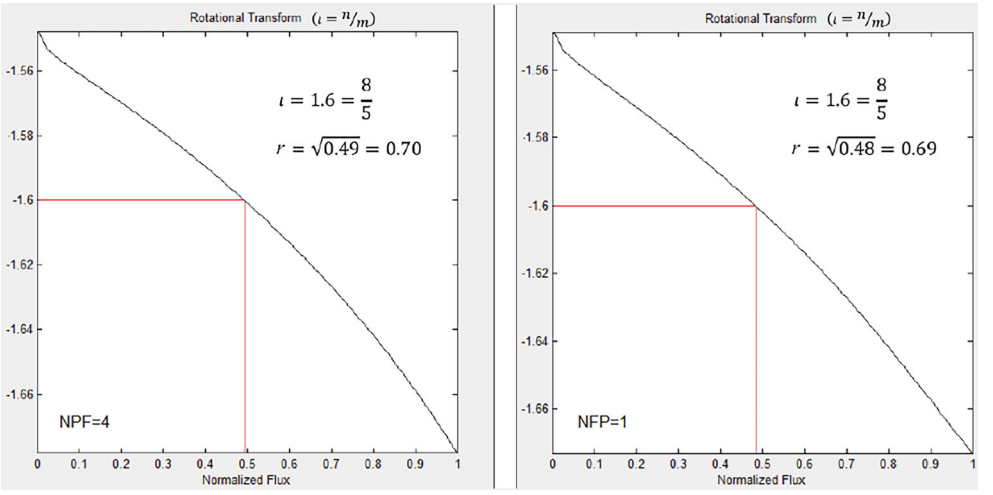

Figure 2. Rotational transform profiles for case A from calculations with four periods (NFP = 4) and a single period (NFP = 1) from VMEC are practically the same.

last configuration, a comparative case was considered for which an inductive current was present which produces a high magnetic shear and some Ohmic heating: this is referred to as Case C. The iota profile for TJ-II is normally quite flat meaning ι does not change much across the radius, as seen in Figure 2 where it varies only in the range (1.55, 1.67). The prominent rational surface in this range is $\iota = 8/5$ which would give rise to islands with 5 poloidal and 8 toroidal periods. This island could be obtained even for the VMEC equilibrium with NFP = 4, since 8 is a multiple of 4. On the other hand, case B has a rotational transform profile ($\iota(s)$) in the range (1.47, 1.57) containing the low-order rational $\iota = 3/2$. The island $m/n = 3/2$ associated with it cannot be obtained from the original equilibrium since 3 is not a multiple of 4 and it is necessary to use the new equilibrium with NFP = 1. The only island that can form in the NFP = 4 case is $m/n = 12/8$, as will be shown later. The interesting feature of high-shear case C is that the $\iota(s)$ range is extended to (1.23, 1.65) and there are several low-order rational surfaces. and many islands can form, as shown in next section.

3. Island formation for arbitrary *n*

Using the equilibria from the three cases mentioned above as input to SIESTA the rational surfaces can resonate with the perturbations introduced and break up into islands. Even though SIESTA considers ideal MHD equilibria, rational surfaces open up by introducing a finite resistivity given externally at a single time-step in order to allow field line slippage. A helical perturbation is introduced with a given poloidal number that has the right periodicity at that rational surface to displace the flux surfaces and form islands. After the surface break-up the ideal MHD evolution is restored until the new equilibrium is reached. For some equilibria, small islands can form even with no helical perturbation (see Section 4) which are then triggered by the numerical noise. In order to visualize the flux surfaces, which are no longer all nested, the field lines are followed with Poincaré plots. The islands are better seen when displayed in radial-poloidal (s, θ) diagrams which is what will be shown in the following. The pressure variation will be shown with pressure isocontours in which the islands

should display by pressure flattening. In order to have reasonable convergence in SIESTA, some parameters have to be adjusted during each run, which for the case of TJ-II is quite tricky given that the equilibrium needs quite a large number of harmonics. The correct combination of parameters can be found for some cases but not for others, as will be seen in the following.

As a first check, we wanted to validate that the code was simulating correctly the full toroidal cycle with no symmetry assumed, So, we ran Case B, which has a rational surface at $\iota = 3/2$, with NFP $= 4$ and with NFP $= 1$. The results are shown in Figures 3 and 4 respectively. In the first case, islands can appear only when the the perturbation resonates as $\iota = m/n = 12/8$, to make n multiple of 4. In Figure 4 there is no restriction on the periodicity of the islands in the toroidal direction, and the island chain with $m = 2$, that was previously unable to grow, can now be seen.

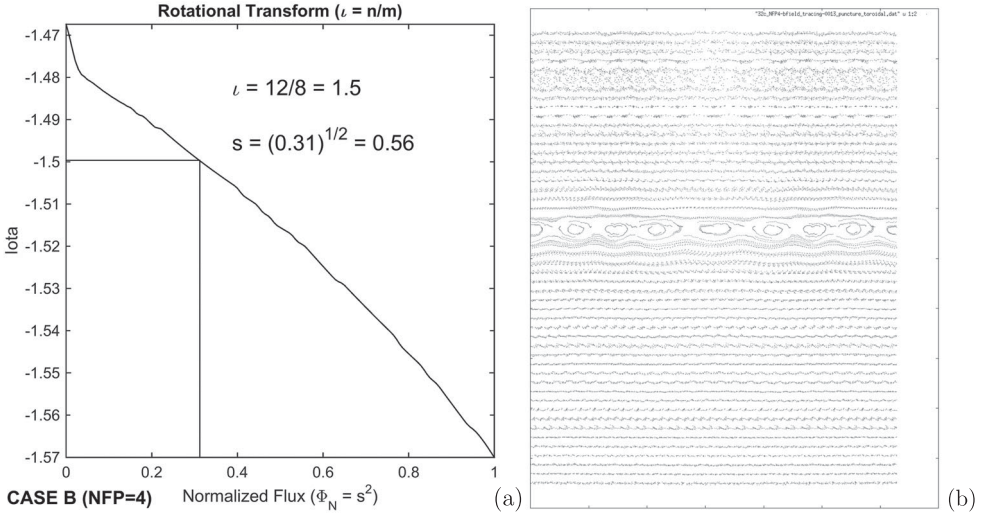

Figure 3. Case B: iota profile and Poincaré plot when field-period = 4.

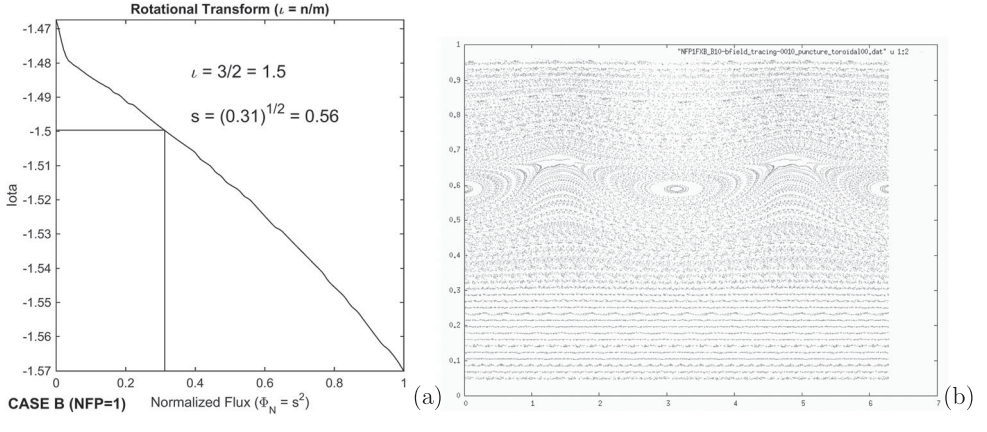

Figure 4. Case B: iota profile and Poincaré plot when field-period = 1.

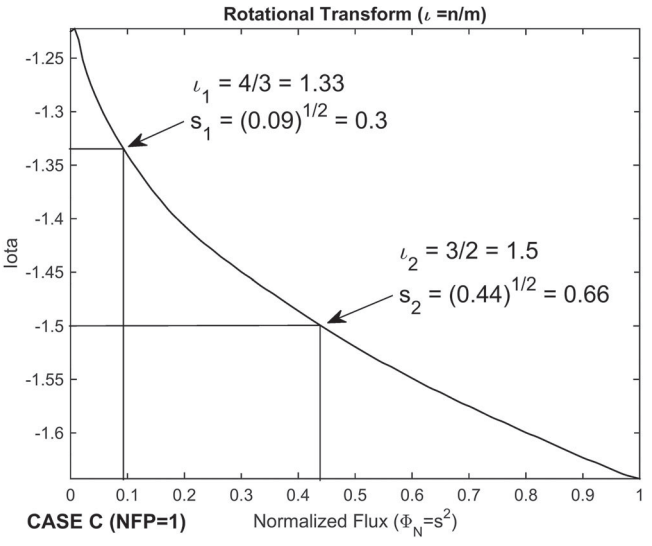

Figure 5. High shear iota profile allowing for $m/n = 3/2, 4/3$ perturbations.

The question of multiple island formation can be addressed analyzing the high-magnetic-shear equilibrium of case C. Figure 5 shows $\iota(s)$ for case C which is seen to include the rational surfaces $\iota = 3/2$ and $\iota = 4/3$. If perturbations with the appropriate mode numbers are given the two magnetic island chains $m/n = 3/2$ and $n/m = 4/3$ could be formed. The equilibrium results from SIESTA presented in Figure 6 indicate that the chains of magnetic islands corresponding to those modes appear around the normalized radial coordinates $s = 0.66$ and $s = 0.30$ respectively. However, the convergence of the variational method with SIESTA is not as good as it was for VMEC; in fact the complex geometry of TJ-II makes very difficult to advance in precision beyond residual forces of 10^{-11} as opposed to 10^{-19} for VMEC. A better test for the convergence is to look for the island effects on the pressure profiles. When convergence is good enough the pressure flattening inside the island should be apparent. This is usually not observed, even when the magnetic field lines show evidence of island formation. The island pressure flattening only develops in equilibria with very small residual forces, and is a sign of a good convergence. Figure 7 shows the pressure isocontours for case C where it is clear that the $m/n = 4/3$ island produced the expected effects on the pressure meaning that island is well formed. On the other hand, the pressure distribution at the rational surface $\iota = 3/2$ did not produce pressure islands, most likely because the residual force of the equilibrium is still not low enough. This probably means that the rational at $\iota = 3/2$ is more robust than the other one. This contention seems to be supported by other studies that have shown that the poloidal periodicity of this surface might not be $m = 2$ but other higher harmonic that resonates at the same surface, like the multiples $\iota = 6/4$, $\iota = 9/6$ or $\iota = 12/8$ (*7*). The mode number was obtained from the observed mode rotation frequency. (See Figure 8).

All those modes were tested by imposing the corresponding perturbations and they produced magnetic islands as can be seen in Figure 8. However, the obtained equilibrium was not good enough to show pressure islands at that surface. This again would indicate that this is a robust rational surface. The rotational transform profile for case C also covers

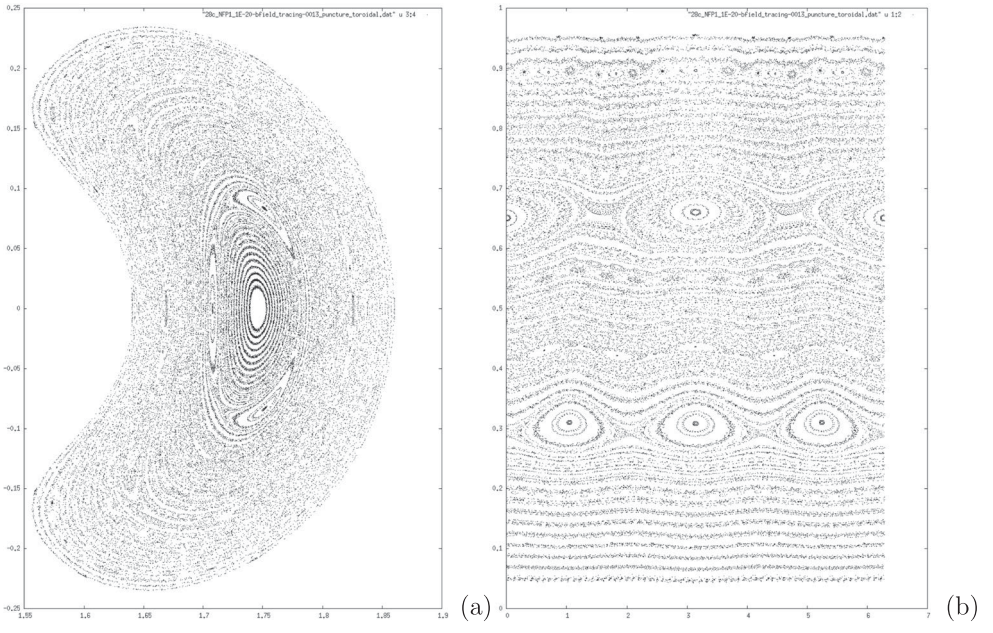

Figure 6. Poincaré plots for high shear case.

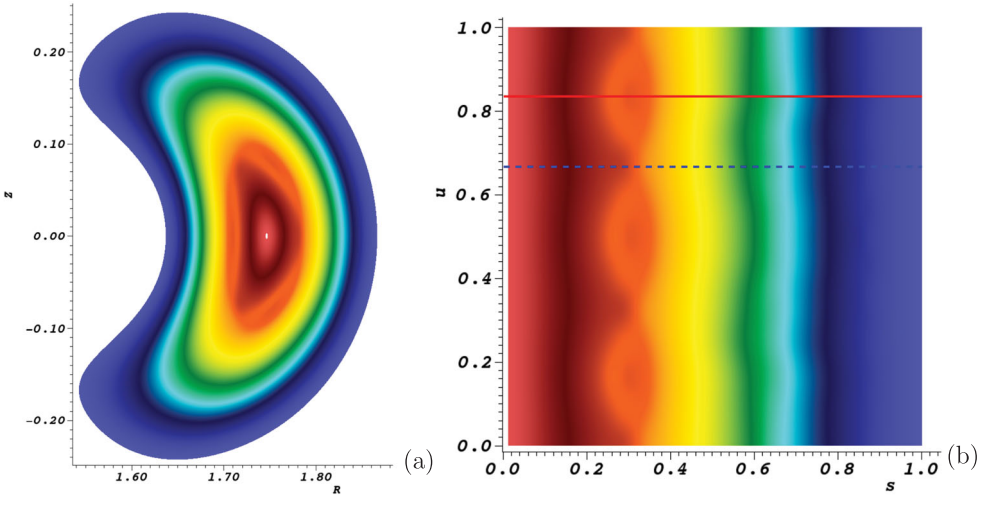

Figure 7. Pressure plots for high shear case; (a) cross section, (b) $s - \theta$ plane.

other rational surfaces near the magnetic axis ($s = 0$) that resonate with the same poloidal frequency, as seen in Figure 8.

The pressure profiles show a bulging of the pressure in the location of rational surfaces, similar to the bulging of the experimental electron pressure observed in other cases of resonant surfaces in TJ-II. An interesting result related to island formation is that it has been found that at the resonant surface $\iota = 8/5$, the heat diffusivity is reduced, which acts as an internal transport barrier, improving the plasma confinement (*3*).

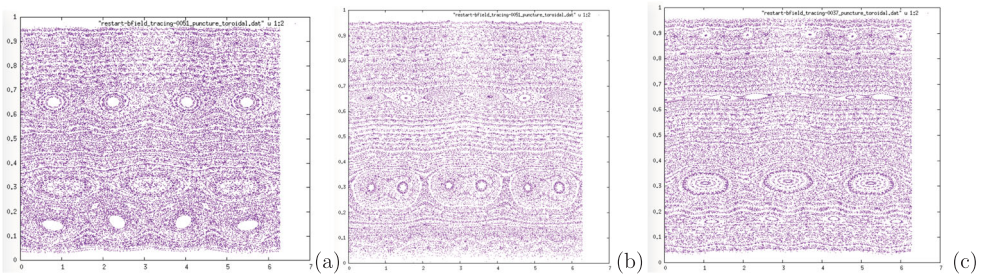

Figure 8. Magnetic surfaces for a second perturbation with $m = 4$ (a), $m = 6$ (b) and $m = 8$ (c).

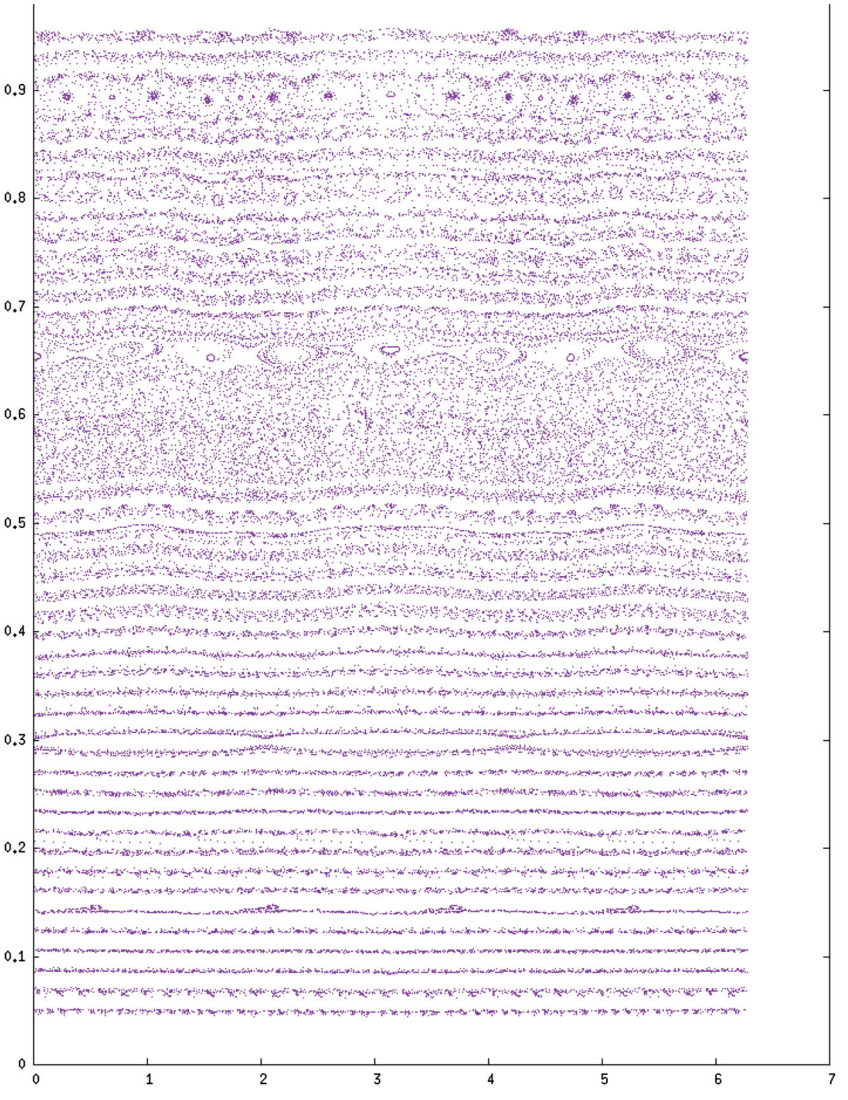

Figure 9. Equilibrium with no initial perturbations for high shear case C. Islands with $m = 8$ at $r = 0.66$ and $m = 3$ at $r = 0.3$ are seen.

4. Unperturbed island formation

It has been mentioned that, in SIESTA, a perturbation with a resonant mode number has to be given in order to break up a rational surface and cause magnetic islands to grow. The island width is usually proportional to the initial perturbation amplitude, up to a certain saturation amplitude. However, in some cases it is also possible to have initial MHD equilibria that can develop islands without an applied perturbation. When Siesta is started with no initial perturbations on the equilibrium of case C a final equilibrium with small magnetic islands is reached. Figure 9 shows that the small island chains are formed at the rationals $\iota = 4/3, 3/2$ with $m = 3$ and $m = 8$, respectively. The seed for island formation may come from numerical noise. This indicates that the equilibrium state from VMEC is inherently unstable to resistive modes for the high shear case.

5. Conclusions

A method was developed to produce magnetic islands with any toroidal periodicity in SIESTA by modifying the way the MHD equilibria are obtained in VMEC for TJ-II. Relevant parameters in SIESTA have to be adjusted in order to achieve good convergence, but due to the complex magnetic geometry of TJ-II the necessary convergence to produce the island effects on pressure was not always found. Further work is required to find the correct simulation parameters to achieve a better convergence at the rational surface $\iota = 3/2$ in order to get the pressure islands. Additionally, it is desirable to identify which poloidal periodicity is more likely to develop at that surface, given that experimental results seem to indicate that high order poloidal modes tend to be dominant. The results obtained with the simulations of VMEC and SIESTA are interesting because they can be related to experimental observations regarding transport barriers. Finding the correct number and positioning of magnetic islands could be the key to achieving better magnetic confinement configurations needed for future fusion reactors. All our computations are done with fixed boundary which the most efficient way of using VMEC and the present SIESTA version only works for this case. However, a free boundary version of SIESTA is now being developed (*8*) and has been tested for the stellarator W7-X in Germany, with satisfactory results. A desirable next step would be to try to get equilibria with islands for free boundary in TJ-II.

Acknowledgments

Helpful discussions with A. López-Fraguas, J.M. Reynolds and D. López-Bruna are gratefully appreciated.

Disclosure statement

No potential conflict of interest was reported by the author(s).

Funding

This work was partially supported by Dirección General de Asuntos del Personal Académico, Universidad Nacional Autónoma de México project DGAPA-UNAM PAPIIT IN112118 and by supercomputo project LANCAD-UNAM-DGTIC-104.

References

(1) López-Bruna, D.; Pedrosa, M.A.; Ochando, M.A.; Estrada, T.; van Milligen, B.P.; López-Fraguas, A.; Romero, J.A.; Baião, D.; Medina, F.; Hidalgo, C. *Plasma Phys. Control. Fusion* **2011,** *53*, 124022.

(2) Ida, K.; Inagaki, S.; Tamura, N.; Morisaki, T.; Ohyabu, N.; Khlopenkov, K.; Sudo, S.; Watanabe, K.; Yokoyama, M.; Shimozuma, T.; Takeiri, Y.; Itoh, K.; Yoshinuma, M.; Liang, Y.; Narihara, K.; Tanaka, K.; Nagayama, Y.; Tokuzawa, T.; Kawahata, K.; Suzuki, H.; Komori, A.; Akiyama, T.; Ashikawa, N.; Emoto, M.; Funaba, H.; Goncharov, P.; Goto, M.; Idei, H.; Ikeda, K.; Isobe, M.; Kaneko, O.; Kawazome, H.; Kobuchi, T.; Kostrioukov, A.; Kubo, S.; Kumazawa, R.; Masuzaki, S.; Minami, T.; Miyazawa, J.; Morita, S.; Murakami, S.; Muto, S.; Mutoh, T.; Nakamura, Y.; Nakanishi, H.; Narushima, Y.; Nishimura, K.; Noda, N.; Notake, T.; Nozato, H.; Ohdachi, S.; Oka, Y.; Osakabe, M.; Ozaki, T.; Peterson, B.J.; Sagara, A.; Saida, T.; Saito, K.; Sakakibara, S.; Sakamoto, R.; Sasao, M.; Sato, K.; Sato, M.; Seki, T.; Shoji, M.; Takeuchi, N.; Toi, K.; Torii, Y.; Tsumori, K.; Watari, T.; Xu, Y.; Yamada, H.; Yamada, I.; Yamamoto, S.; Yamamoto, T.; Yoshimura, Y.; Ohtake, I.; Ohkubo, K.; Mito, T.; Satow, T.; Uda, T.; Yamazaki, K.; Matsuoka, K.; Motojima, O.; Fujiwara, M. *Nucl. Fusion* **2004,** *44,* 290.

(3) López-Bruna, D.; Vargas, V.I.; Romero, J.A. *J. Physics: Conf. Ser.* **2015,** *591*, 012013.

(4) López-Bruna, D.; Ochando, M.A.; López-Fraguas, A.; Medina, F.; Ascasíbar, E. *Nuclear Fusion* **2013,** *53*, 073051.

(5) Hirshman, S.P. *Phys. Fluids* **1983,** *26*, 3553.

(6) Hirshman, S.P.; Sanchez, R.; Cook, C.R. *Phys. Plasmas* **2011,** *18*, 062504.

(7) Ochando, M.A.; López-Bruna, D.; Pedrosa, M.A.19th ISHW - 16th IEA-RFP workshop (2013), Padova, Italy

(8) Peraza-Rodriguez, H.; Reynolds-Barredo, J.M.; Sanchez, R.; Geiger, J.; Tribaldos, V.; Hirshman, S.P.; Cianciosa, M. *Phys. Plasmas* **2017,** *24*, 082516.